ACS APPLIED MATERIALS & INTERFACES

www.acsami.org

Research Article

Regulating Tissue-Mimetic Mechanical Properties of Bottlebrush Elastomers by Magnetic Field

Sergei A. Kostrov, Erfan Dashtimoghadam, Andrew N. Keith, Sergei S. Sheiko,* and Elena Yu. Kramarenko*

Cite This: https://doi.org/10.1021/acsami.1c12860

Read Online

ACCESS | Metrics & More | Article Recommendations | Supporting Information

ABSTRACT: We report on a new class of magnetoactive elastomers (MAEs) based on bottlebrush polymer networks filled with carbonyl iron microparticles. By synergistically combining solvent-free, yet supersoft polymer matrices, with magnetic microparticles, we enable the design of composites that not only mimic the mechanical behavior of various biological tissues but also permit contactless regulation of this behavior by external magnetic fields. While the bottlebrush architecture allows to finely tune the matrix elastic modulus and strain-stiffening, the magnetically aligned microparticles generate a 3-order increase in shear modulus accompanied by a switch from a viscoelastic to elastic regime as evidenced by a ca. 10-fold drop of the damping factor. The developed method for MAE preparation through solvent-free coinjection of bottlebrush melts and magnetic particles provides additional advantages such as injection molding of various shapes and uniform particle distribution within MAE composites. The synergistic combination of bottlebrush network architecture and magnetically responsive microparticles empowers new opportunities in the design of actuators and active vibration insulation systems.

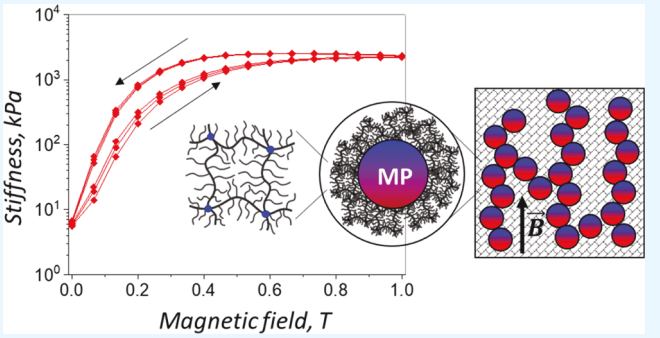

KEYWORDS: *bottlebrushes, magnetoactive elastomers, mechanical properties, magnetorheological effect, damping factor*

INTRODUCTION

Regulating the mechanical properties of soft materials is vital for many applications such as biomedical devices and soft robotics. The regulation tools include both the inherent material structure and external stimuli. Particularly vital are tissue-mimetic materials made of different types of polymer networks such as elastomers and gels that possess a diverse arsenal of architectural tools for tuning their mechanical characteristics. In linear polymer networks, the elastic shear modulus is largely controlled by the degree of polymerization (DP) of the network strand (n_x) and the DP of the entanglement strand (n_e) as $G \cong \rho k_B T(n_x^{-1} + n_e^{-1})$, where ρ is the number of monomeric units per unit volume. This equation sets a lower limit for modulus as $G \cong \rho k_B T n_e^{-1} \cong 10^5$ Pa due to inherent chain entanglements that preclude soft elastomers with $G < G_e \cong 10^5$ Pa. To circumvent this issue, different routes have been explored including (i) cross-linking of semidilute solutions, (ii) under-cross-linking, and (iii) swelling networks with a solvent. Routes (i) and (ii) deliver loose networks with an ill-defined topology and a low gel fraction. Although route (iii) allows for an accurate modulus control, the liquid fraction leaches both spontaneously and under deformation, which limits practical applications and represents a significant health hazard when implanted in the body.

Recently, we have reported a different approach to the design of supersoft elastomers based on polymer networks with brushlike strands.[1] By controlling the side chain length and the grafting density, we can precisely vary the elastic shear modulus within an unprecedented range from 10^2 of fat tissue to 10^6 Pa of skin without adding solvent as a material softener.[2,3] This modulus reduction below the linear chain entanglement limit ($G_e \cong 10^5$ Pa) is achieved due to architectural disentanglement of bottlebrush network strands, which allows synthesizing networks with an extremely low cross-link density.[4] An important distinction of this approach is that prepared networks are solvent-free and therefore do not leach.

These supersoft nonleaching elastomers represent an ideal matrix for the design of composite materials. Particularly interesting are magnetoactive elastomers (MAEs) prepared by mixing polymer networks and magnetic particles (MPs) (Figure 1), which allow for external regulation of the material

Received: July 7, 2021
Accepted: July 26, 2021

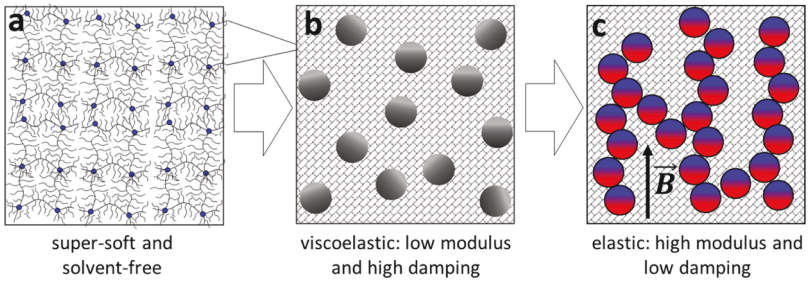

Figure 1. Schematic representation of the structure of (a) a bottlebrush network as a matrix for MAEs. (b) MAE with a homogeneous distribution of MPs demonstrating a relatively low modulus and a high viscoelasticity. (c) External magnetic field ($\vec{B}$) causes magnetization and alignment of magnetic filler particles within the soft matrix. Dual control of stress−strain behavior of an MAE is achieved *via* (i) tuning the architecture of the bottlebrush network and MP concentration and (ii) externally applied magnetic field, which modulates not only the MAE elastic modulus within a range of 3 orders of magnitude but also its viscoelastic response.

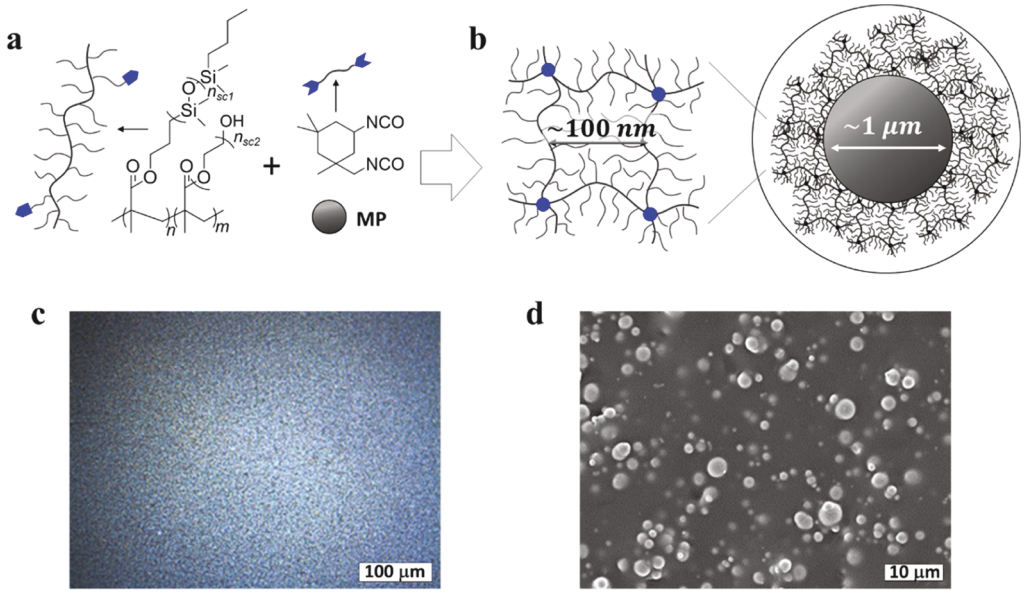

Figure 2. (a) Synthesis of solvent-free MAEs by coinjecting random PDMS-*r*-PEG brush copolymers with a controlled fraction of end-functionalized PEG side-chains, a di-isocyanate cross-linker, and MPs. (b) Schematic representation of a multiscale structure of a bottlebrush magnetic elastomer, where the bottlebrush network provides a supersoft matrix for micrometer-sized MPs. A mesh size estimate of ∼100 nm corresponds to an upper limit defined by the strand contour length $R_{max} \cong n_x l$, where $n_x \cong 400$ is the DP of the backbone and $l = 0.25$ nm is the monomer length. (c) Optical and (d) SEM micrographs of a MAE 1.5−20 sample display homogeneous particle distribution. The particle size in (d) is consistent with the average particle size of 4.5 μm provided by the vendor.

mechanical properties and shape actuation.[5−9] Depending on the magnetic field, matrix modulus, and MP concentration, the MAE stiffness could be amplified by $\sim 10^2-10^4$ times.[10−12] In other words, an elastomer with a modulus of $\sim 10^2$ Pa (fat tissue) can be readily converted to a skinlike material with a modulus of 10^6 Pa after applying a magnetic field. Furthermore, magnetic fields also affect the viscoelastic response, which enables the development of active vibration damping systems.[13,14] The origin of this extraordinary magnetorheological (MR) effect lies in the field-induced MP magnetization and alignment within the polymer matrix,[15−17] whereby softer matrices allow for larger particle displacements leading to a larger MR effect.[9,11,12,16] Thus, the significant advancements in enhancing the MR effect have traditionally been achieved by softening the matrix through large quantities of silicone oil additive (up to 70 vol %), which is prone to leaching, and thus significantly limit the applicability of such materials. Herein, we explore the MR potential of solvent-free, yet supersoft polydimethylsiloxane (PDMS) bottlebrush elastomers that alleviate many problems associated with leaching gels while providing more leverage for mechanical property control. The inert and nonleaching nature of PDMS make these magnetic composites suitable for biomedical applications such as treatment of retinal detachment[18,19] and substrates with externally modulated stiffness for cell differentiation.[20]

RESULTS AND DISCUSSION

Synthesis of Bottlebrush MAEs. MAEs were prepared by coinjecting mixtures of PDMS-*r*-polyethyleneglycol (PEG) brush melt, a difunctional cross-linker [isophorone diisocyanate (IPDI)], a catalyst (dibutyltin dilaurate, DBTL), and different mass concentrations of MPs (Figure 2). To ensure the long-term shelf life and injectability of the MAE formulations, a dual-barrel syringe with a static mixer nozzle was used to inject and cast them. PDMS-*r*-PEG melt, MPs, and DBTL (400 ppm) were thoroughly mixed and loaded into one barrel, while the other barrel contained the mixture of PDMS-*r*-PEG melt and IPDI (at NCO/OH molar ratio of 1:1). Subsequently, the mixtures were coinjected into Teflon molds

https://doi.org/10.1021/acsami.1c12860
ACS Appl. Mater. Interfaces XXXX, XXX, XXX−XXX

and cured at an elevated temperature. MPs used in this work were magnetically soft carbonyl iron (CI) spherical particles with the average diameter of 4.5 μm (grade R-20, OOO SINTES-PKG, Russia). Specific magnetization and coercivity of these MPs are equal to 190 ± 8 emu/g and 9 ± 3 Oe, respectively.[21] Bottlebrushes were synthesized by atom transfer radical copolymerization of PDMS−methacrylate macromonomers (n_{sc} = 14) and PEG−methacrylate macromonomers (n_{sc} = 12) with hydroxyl (OH^-) chain ends,[22] which are then cured into elastomers at 60 °C using a di-isocyanate cross-linker (IPDI) (Figures 2a and S1−S3). The uniformity of PEG incorporation was monitored by NMR (Figure S4). We prepared three series of bottlebrush networks with different cross-link densities regulated by the incorporation of OH-terminated side chains (series 1: 0.5 mol %, series 2: 1.0 mol %, and series 3: 1.5 mol %). For each of the three bottlebrush network series, we prepared MAEs containing 1.4, 3.0, 11.1, and 22.5 vol % of CI microparticles with an average size of 4.5 μm by coinjecting with bottlebrush/cross-linker formulations (Table 1). Figure 2b schematically shows the multiscale

Table 1. MAE Mechanical Properties for Different Cross-link Densities and MP Volume Fractions

sample[a]	MP vol %[b]	E (kPa)[c]	E_0 (kPa)[d]	β[e]	λ_{max}[f]	$\lambda_{max,th}$[g]	σ_{max} (kPa)[h]
0.5−0	0	1.00	1.08	0.05	4.1	4.3	9.1
0.5−1	1.4	1.17	1.18	0.07	4.0	3.9	11.4
0.5−3	3.0	1.15	1.29	0.08	4.9	3.5	28.1
0.5−10	11.1	1.15	1.34	0.10	5.6	3.1	86.8
0.5−20	22.5	1.8	2.9	0.28	3.8	1.9	103.1
1.0−0	0	6.9	8.6	0.15	2.3	2.6	17.8
1.0−1	1.4	7.1	9.4	0.18	2.3	2.4	24.7
1.0−3	3.0	4.6	10.4	0.41	2.1	1.6	26.6
1.0−10	11.1	3.5	12.6	0.55	2.8	1.4	93.7
1.0−20	22.5	1.3	18.5	0.78	2.3	1.1	104.3
1.5−0	0	9.5	15.8	0.29	1.8	1.9	17.5
1.5−1	1.4	9.3	17.4	0.30	1.7	1.8	19.4
1.5−3	3.0	14.2	24.7	0.31	1.7	1.8	22.9
1.5−10	11.1	0.56	53.9	0.92	1.3	1.1	30.6
1.5−20	22.5	0.10	111.1	0.98	1.2	1.0	38.9

[a]The first number in the sample name indicates the molar fraction of OH-terminated side chains defining the cross-link density, while the second number stands for the volume concentration of iron MPs. For instance, sample 0.5−10 contains 0.5 mol % of OH-groups and 11.1 vol % of MPs. [b]MP volume fraction calculated from the mass fraction using PDMS density 0.97 g/cm^3 and CI density 7.8 g/cm^3. [c]Structural modulus (eq 2). [d]Young's modulus (eq 4). [e]Firmness parameter (eq 3) obtained by fitting the stress−strain curves in Figure 3 with eq 1 (Figure S6). [f]Experimental and [g]Theoretical elongations at break where $\lambda_{max,th} \cong \sqrt{\beta^{-1}}$ (eq 3). [h]True stress at break.

structure of the obtained MAE composites. While the bottlebrush architecture of network strands (~100 nm) defines the mechanical properties of the MAE matrix,[1] introducing MPs creates magneto-mechanical coupling on the micron scale (Figure 1c). As such, the bottlebrush matrix may be viewed as a continuum medium with viscoelastic properties molecularly encoded by brush architecture.

Network formation was monitored in situ by measuring the storage (G') and loss (G'') moduli, where the curing time was identified at the crossover of the $G'(t)$ and $G''(t)$ curves (Figure S5). Given the large size of bottlebrush macromolecules, the minuscule fractions of cross-linking moieties (0.02 mol %) enable fully conjugated networks without polymerization-induced MAE shrinkage. For each sample, the gel fraction was measured to be within 95−98 wt %, indicating that the synthesized MAEs contain less than 5 wt % liquid fraction, which is significantly lower than 70 wt % of the current state-of-the-art gel-based MAEs. The remaining 2−5 wt % liquid fraction is composed of large brushlike macromolecules with limited mobility.

Mechanical Properties of Bottlebrush MAEs. Figure 3a−c shows the stress−strain response to uniaxial elongation of bottlebrush elastomers with different cross-link densities and MP concentrations. Some composites closely replicate the deformation response of assorted tissues (Figure 3d). The deformation response of polymer networks with semiflexible strands is described by two mechanical characteristics: (i) Young's modulus E_0, which characterizes elastomer stiffness at small deformations ($\lambda \to 1$) and (ii) firmness parameter β, which describes the modulus increase with deformation. For conventional linear chain elastomers with flexible strands, the strain-stiffening effect is negligible ($\beta \cong 0$). In contrast, the semiflexible nature of bottlebrush strands demonstrates a significant stiffness enhancement ($\beta \cong 0.1$) visualized by a strong curvature of the stress−strain curves (Figure 3a). To extract E_0 and β from the stress−strain curves, we fitted the curves with a proven equation of state relating true stress σ_{true} with the network elongation ratio $\lambda = L/L_0$ from its initial L_0 to deformed size L[23]

$$\sigma_{true} = \frac{E}{9}(\lambda^2 - \lambda^{-1})\left[1 + 2\left(1 - \frac{\beta(\lambda^2 + 2\lambda^{-1})}{3}\right)^{-2}\right] \quad (1)$$

which is defined by

$$E \cong k_B T\varphi/(\nu n_x) \quad (2)$$

$$\beta = \langle R_{in}{}^2\rangle / R_{max}{}^2 \cong \lambda_{max,th}{}^{-2} \quad (3)$$

$$E_0 = \left.\frac{\partial \sigma_{true}}{\partial \lambda}\right|_{\lambda \to 1} = \frac{E}{3}\left(1 + \frac{2}{(1-\beta)^2}\right) \quad (4)$$

where E is the structural modulus controlled by the cross-link density $\sim\varphi n_x{}^{-1}$, which is defined by n_x, the DP of the bottlebrush backbone between two junctions, and $\varphi \cong n_g/(n_g + n_{sc})$, the molar fraction of the backbone within a bottlebrush strand with DPs of side chains n_{sc} and backbone spacer between neighboring side chains n_g; $\langle R_{in}{}^2\rangle \cong R_{max} b$ and $R_{max}{}^2$ are the mean-square end-to-end distance and the square of the contour length of bottlebrush network strands, respectively. The strand flexibility is characterized by the Kuhn length b. Note that β is inversely proportional to the square of the maximum theoretical elongation of network strands ($\lambda_{max,th} \cong R_{max}/\sqrt{\langle R_{in}{}^2\rangle}$), and it has the same physical meaning as the finite extensibility parameter used in constitutive equations for rubbers introduced in the Ogden, Fung, and Gent models.[23] Yet, there is an important distinction: Unlike the previously developed phenomenological models, the parameter β is directly related to the DP and the persistence length of network strands (eq 3). For linear elastic materials (the firmness parameter $\beta \ll 1$), the structural and Young's moduli are equal (eq 4). However, in elastomers with nonlinear deformation response ($\beta \sim 0.1-1$), the Young's modulus is much higher than the structural modulus and largely controlled by β. Equation 1 was tested for various

https://doi.org/10.1021/acsami.1c12860
ACS Appl. Mater. Interfaces XXXX, XXX, XXX−XXX

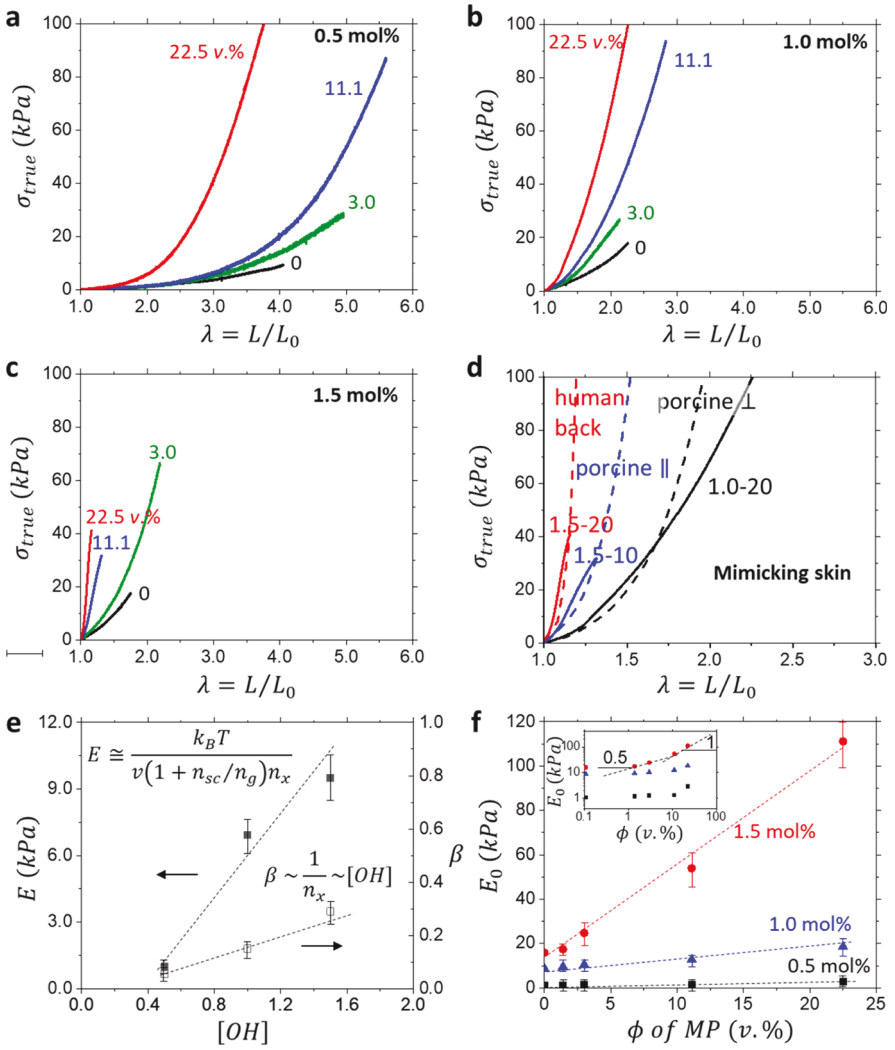

Figure 3. (a–c) Stress–strain curves of bottlebrush elastomers with different cross-link densities and fractions of MPs (as indicated). The less cross-linked samples [(a) 0.5 mol % of OH] are softer and more extendable. (d) MAEs with high MP concentrations (as indicated) closely replicate the deformation response of assorted skin tissues.[2] This is ascribed to the significant increase of the firmness parameter β with the MP concentration (Table 1). The parallel (∥) and perpendicular (⊥) directions for porcine skin tests refer to the so-called Langer's lines corresponding to the dominant axis of mechanical tension in the tissue.[25] (e) Both the structural modulus (E) and firmness parameter (β) increase with the cross-link density $\sim((1 + n_{sc}/n_g)n_x)^{-1}$, which is proportional to the molar fraction of the OH end groups [OH]. (f) Young's modulus of the synthesized MAEs increases with the MP volume fraction. The increase is nonlinear as seen in the corresponding log–log plot (insert). The error bars are obtained from multiple (at least 5 times) tensile tests of the same material.

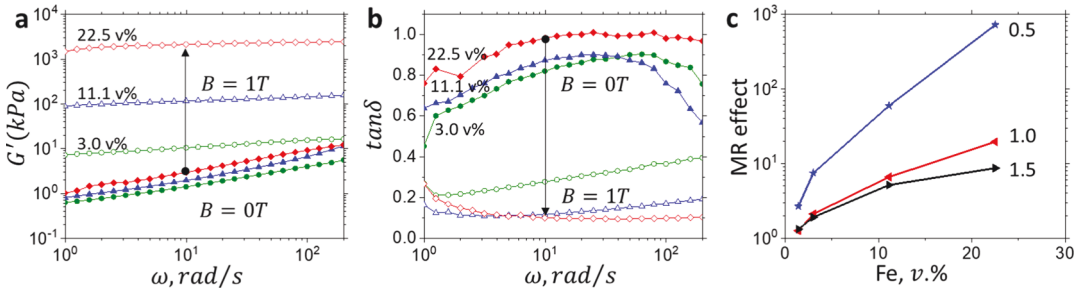

Figure 4. Frequency dependences of (a) the storage modulus, G', and (b) the loss factor, **tan** δ, of MAE-0.5–x series containing various amounts of the magnetic CI particles (as indicated) measured at B = 0 (filled symbols) and B = 1 T (open symbols). The storage modulus at B = 0 T measured at the lowest frequency of 1 rad/s shows a good agreement with the Young's modulus (Table 1) as $E_0 \cong 3G'$ assuming the Poisson ratio of 0.5 (Figure S9). (c) Dependence of the MR effect of MAEs with different concentrations of PDMS–OH side chains on the volume fraction of the ferromagnetic filler at the oscillation frequency of 10 rad/s.

polymer networks and showed a better agreement with the experiment than other nonlinear elasticity models.[23]

Table 1 summarizes the obtained mechanical characteristics of neat bottlebrush elastomers with different cross-link

https://doi.org/10.1021/acsami.1c12860
ACS Appl. Mater. Interfaces XXXX, XXX, XXX–XXX

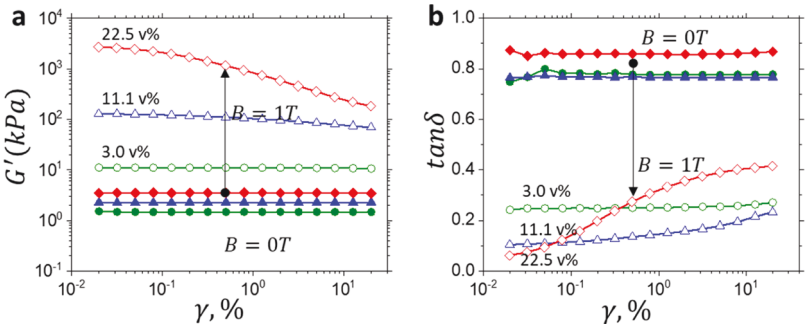

Figure 5. Dependence of the (a) storage modulus, G', and (b) loss factor, **tan** δ, of MAEs with 0.5% of PEG-OH side chains and different volume fractions of MPs (as indicated) on the strain amplitude measured at B = 0 T (filled symbols) and in a magnetic field B = 1 T (open symbols).

densities and their composites with different MP fractions. As shown in Figure 3e, decreasing the cross-link density results in progressive softening and firmness decrease of MAE matrices as $E \sim \varphi n_x^{-1}$ and $\beta \sim n_x^{-1}$, respectively. We achieved the Young's modulus as low as 1 kPa, which is ca. 100 times softer than linear chain PDMS elastomers and closely matches the modulus of soft biological tissues such as lung, kidney, and brain.[24] Upon adding MPs, the modulus increased with the MP volume fraction (Figure 3f), yet the MAE composites remain relatively soft with E_0 < 100 kPa, that is, within the biological softness range (Figure 3d).

Viscoelastic Properties in Magnetic Field. The magnetic response of the bottlebrush MAEs was examined by in situ dynamic mechanical analysis in the presence of a magnetic field. As an example, Figure 4 depicts the response of the softest MAE-0.5−x with different MP fractions (Supporting Figure S8 for the MAEs with higher cross-link densities). Without a magnetic field, the storage modulus G' slightly grows with an increase of the magnetic filler content, which is consistent with the data obtained by tensile tests (Table 1). The loss factor, tan δ, exhibits less consistent behavior due to the interplay of the particle-enhanced stiffening of brush networks (β increase in Table 1) and increasing friction between the polymer matrix and microparticles (Figure S8b,d). Yet, for all compositions, tan $\delta \cong 1$, which characterizes a strong viscoelastic response and significant damping in a broad frequency range.

In a magnetic field of B = 1 T, all samples demonstrate a significant MR effect, which can be summarized by (i) up to 3 orders of magnitude modulus increase (Figure 4a) and (ii) up to 10-fold damping decrease (Figure 4b). Even at a small MP fraction of 3 vol %, we observe an almost 10× increase of G'. The largest MR effect of almost 1000× (10^5%) stiffness augmentation is demonstrated by the composite containing 22.5 vol % of magnetic microparticles. The growth of G' is caused by long-range interactions of magnetized particles enhanced by their assembly into chainlike structures aligned along the field lines.[7] Remarkably, the magnetic field allows transforming strongly viscoelastic materials characterized by tan $\delta \cong 1$ to highly elastic ones with tan $\delta \cong 0.1$. Note that G'' also increases in the magnetic field, yet much slower than G', resulting in the overall elastic response as evidenced by the plateau behavior of G' weakly depending on the shear frequency (Figure 4a). The MR effect can be quantified as $\Delta G' = G'_{max}/G'_0$, where G'_0 is the initial value of the modulus in the absence of a magnetic field and G'_{max} is the storage modulus measured at B = 1 T. As shown in Figure 4c, the effect is higher for matrices with lower cross-link densities and higher MP fractions. The largest MR effect is demonstrated by MAE-0.5−20, reaching typical values for conventional MAEs that contain up to 70 vol % of potentially leachable low-molecular-weight plasticizers.[7,10−13] Both increasing G' and decreasing tan δ provide various damping mechanisms depending on a specific application. For example, tuning stiffness of an MAE element in a magnetic field causes shifts in both the resonance frequency and energy dissipations. The field-dependent shear modulus G' of MAEs gives great opportunities for the development of both semiactive vibration control in flexible structures and actively controllable vibration absorbers and vibration isolators by using sandwich-like structures.[14]

It should be noted that in contrast to conventional MAEs, bottlebrush elastomers demonstrate a strongly nonlinear elastic response, whereby a slight extension of network strands causes a dramatic stiffness increase, which considerably reduces the MR effect. Due to steric repulsion between densely grafted side chains, bottlebrush elastomers are in the finite extensibility regime where mechanical properties depend nonlinearly on the cross-link density. The Young's modulus (as well as shear modulus) depends on two parameters: the structural modulus E and the firmness parameter β (eq 4). The latter becomes dominating at a high filler concentration. Specifically, the 1.5−20 sample shows the extremely high value of β = 0.98, which suggests that network strands are highly extended (eq 3). The resulting strain-stiffening effect significantly hinders the motion and rearrangement of MPs in the magnetic field. This hindering is nonlinear and becomes more visible at higher cross-link densities. A higher mobility of MPs in the softest series 0.5 is seen on the magnetization curves presented in Figure S8, where the opening of the hysteresis loop and the magnetization values in the range of magnetic fields, in which rheological measurements were performed, are greater for the MAE-0.5−x samples. It should also be mentioned that in conventional gel-based MAEs, rearrangement of MPs is facilitated by the presence of a low-molecular-weight diluent, which however may lead to significant composition fluctuations during particle rearrangement.

Strain Dependence of the Dynamic Modulus. Filled rubbers typically demonstrate a shear-thinning behavior, which is known as the Payne effect and is attributed to breaking of filler particle aggregates with an increasing mechanical strain.[26−32] A magnetic counterpart of the Payne effect (so-called "magnetic Payne effect") was initially introduced to describe the strain softening in magnetic fields due to disruption of long-range interactions between magnetized particles in swollen gels.[27] An order of magnitude drop of the storage modulus was observed for soft MAEs based on

https://doi.org/10.1021/acsami.1c12860
ACS Appl. Mater. Interfaces XXXX, XXX, XXX−XXX

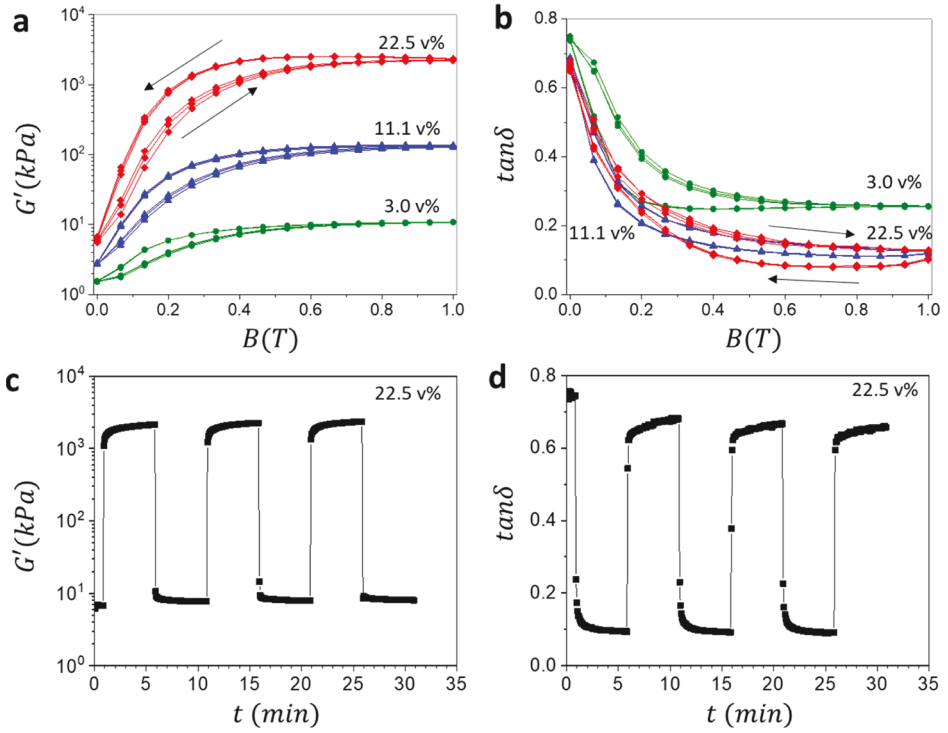

Figure 6. Hysteresis of (a) storage modulus, G', and (b) loss factor, **tan δ**, of MAEs with 0.5% of PDMS-OH side chains in the ascending/descending magnetic field. Time dependence of (c) the storage modulus and (d) loss factor upon stepwise switching on-and-off of the magnetic field B = 1 T with 5 min interval for each state. All measurements were performed in the linear viscoelastic regime at the strain amplitude of 0.1 and a fixed oscillation frequency of 10 rad/s.

conventional linear PDMS matrices containing large quantities of liquid plasticizers.[31,32] Figure 5 depicts the dependences of the storage modulus and the loss tangent of the bottlebrush MAE-0.5−x series on the strain amplitude both in the absence of a magnetic field and at B = 1 T (see Figure S10 for MAEs with a higher cross-link density). Without a magnetic field, all samples demonstrate a weak Payne effect, that is, both the storage modulus and loss factor remain nearly constant up to a shear strain of 20%. However, the behavior drastically changes in the magnetic field due to the emergence of the magnetic Payne effect, with the strongest response demonstrated by the softest MAE-0.5−20 sample. Disruption of the magnetic filler network causes not only a significant drop of G' but is also accompanied by considerable energy dissipations resulting in an increasing tan δ at large strains. At lower fractions, the effect is less significant.

Hysteresis of Viscoelastic Properties of MAEs in Magnetic Fields. Figure 6 demonstrates the reversibility and responsiveness of MAE-0.5−x samples in cyclic magnetic fields. All samples show the characteristic S-shaped $G'(B)$ dependences and well-pronounced hysteresis that become more apparent at higher cross-link densities (Figure S11) and using log−log presentation. Both behaviors are typical for MAEs and are attributed to a complex interplay between elastic and magnetic interactions.[33−35] At low magnetic fields, polymer network elasticity dominates, and a slight modulus increase is due to induced long-ranged magnetic interactions between filler particles. At intermediate fields, where major changes of viscoelastic properties take place, increasing magnetic forces overcome the elasticity to cause filler rearrangements. At higher fields, any further particle reorganizations are hampered by strong magnetic couplings, a dense packing of particles within aggregates aligned with the field, and saturation of particle magnetization, which also tends to result in modulus saturation. The hysteresis is attributed to strong magnetic couplings between MPs in a strong field, which is perturbed by restoring elastic forces upon dropping the magnetic field below some critical value. Indeed, the hysteresis is the most pronounced for the softest MAE-0.5−20 containing the largest quantity of MPs because in this case, magnetic interactions dominate in a wider range of B. To demonstrate the responsiveness and resilience of bottlebrush MAEs in a magnetic field, a series of periodic 1 T ramps were applied. As shown in Figure 6c,d, our MAEs promptly respond to the on−off field alterations while maintaining both the original and induced mechanical properties.

CONCLUSIONS

The combination of bottlebrush network architecture and magnetically responsive microparticles empowers synergistic enhancement on MAE performance both with and without the presence of a magnetic field. Although the bottlebrush network architecture allows to finely tune the MAE mechanical properties in a broad range,[1−3] incorporation of microparticles also significantly affects the deformation response even without a magnetic field. Indeed, the particle-filled bottlebrush elastomers demonstrate concurrent enhancement of both modulus and firmness, which allows mimicking the stress−strain response of assorted skin tissues. In the presence of a magnetic field, additional control over MAE's mechanical properties enables not only 1000× stiffness enhancement but also fundamentally changes the viscoelastic nature of bottlebrush MAEs due to almost 10-fold decrease of the damping factor. Effectively, materials switch from being strongly viscoelastic with significant energy dissipation (tan δ

https://doi.org/10.1021/acsami.1c12860
ACS Appl. Mater. Interfaces XXXX, XXX, XXX−XXX

≅ 1) to strongly elastic with tan $\delta \cong 0.1$, which is vital for the design of active vibration absorbers.[13,14] This level of the MR effect can be obtained for MAEs based on traditional linear PDMS matrices only by adding up to 70 vol % of the liquid plasticizer, which deteriorates MAE performance characteristics. In contrast, the supersoft bottlebrush composites cured through the injectable solvent-free strategy neither leaches spontaneously nor upon actuation as the grafted side chains are chemically connected to network strands. This significantly improves the MAEs' longevity and expands the range of their practical applications as this approach (i) enables controlled cross-linking, (ii) hinders particle sedimentation during elastomer curing, and (iii) even permits 3D printing desired shapes.

The bottlebrush MAEs are also both resilient and responsive. In contrast to conventional filled rubbers, the bottlebrush MAEs maintain a linear viscoelastic response in a wide range of strain amplitudes up to 20% and promptly responds to periodic on−off switching of the magnetic field. Similar to traditional MAEs, bottlebrush magnetic composites demonstrate the Payne effect as well as considerable mechanical hysteresis in magnetic fields. The observed hysteretic behavior in external magnetic fields is an intrinsic attribute of MAEs as a result of a combination of different energy dissipation mechanisms taking place at different length scales caused by restructuring of the magnetic filler.[7] Various compensation schemes developed for other stimuli-responsive materials exhibiting relaxation phenomena can readily be generalized and applied to MAE devices.[36]

EXPERIMENTAL SECTION

Rheology. Viscoelastic properties of MAEs were studied using a rheometer (Anton Paar, model Physica MCR 302) equipped with the magnetic cell MRD 170/1 T. Measurements of the components of the complex shear modulus of the samples were performed in the plate−plate geometry in the dynamic mode under harmonically oscillating shear stress. For this, disklike samples with a diameter of 14 mm were cut out of a MAE ribbon having a thickness 1 mm deposited on a film substrate. A removable measuring head of the rheometer was brought to contact with the upper sample surface, and the sample was stuck to it due to a strong adhesion. After that, the film was removed from the bottom surface of the sample using a spatula, and the measuring head with the sample was fixed in the rheometer. The upper plate underwent forced torsion oscillations with the strain γ changing according to the harmonic law $\gamma = \gamma_0 \sin(\omega t)$, where γ_0 is the strain amplitude and ω is the angular frequency. The frequency and amplitude of the external strain were varied, and dependencies of the storage modulus G', the loss modulus G'', and the loss factor, defined as $\tan \delta = G''/G'$, on the oscillation frequency, strain amplitude, as well as the magnetic field were obtained for all samples. Frequency tests were carried out in the linear viscoelastic regime at the strain amplitude $\gamma_0 = 0.1$ in the frequency range 1−100 rad/s. Amplitude tests were performed at the fixed oscillation frequency $\omega = 10$ rad/s in the range $\gamma_0 = 0.0002$−0.2. In most of the tests, the temperature was kept constant equal to 20 °C.

Magnetic flux density B within the measuring unit was controlled by the driving current produced by the electromagnet and was varied in the range 0−1 T. The magnetic field was applied perpendicular to the shearing plane of the sample.

Uniaxial Tensile Tests. Dogbone-shaped samples with bridge dimensions of 12 mm × 2 mm × 1 mm were loaded to a RSA-G2 DMA (TA Instruments) dynamic mechanical analyzer and subjected to uniaxial elongation at 20 °C and a constant strain rate of 0.005 s^{-1}. For each sample, tests were conducted at least five times to reproducibility and standard error of the elastic modulus within 10%. The elongation ratio λ for uniaxial network deformation is defined as the ratio of the sample's instantaneous size L to its initial size L_0, $\lambda = L/L_0$. The true stress is calculated by multiplying the engineering stress with the elongation ratio as $\sigma_{true}(\lambda) = \sigma_{eng}(\lambda)\lambda$, which accounts for the decrease of the sample cross-section area, assuming that elastomers do not change volume upon deformation. The structural modulus E and the strain-stiffening parameter β are obtained by fitting $\sigma_{true}(\lambda)$ curves with eq 1 (Figure S6). The Youngs modulus can be either calculated using eq 4 or measured directly as a $\sigma_{true}(\lambda)$ slope at $\lambda \to 1$ (Figure S9a). All stress−strain curves show dependence of the true stress, σ_{true}, on the elongation ratio $\lambda = L/L_0$ in accordance with eq 1.

ASSOCIATED CONTENT

Supporting Information

The Supporting Information is available free of charge at https://pubs.acs.org/doi/10.1021/acsami.1c12860.

Monitoring polymerization kinetics by NMR and characterization of the mechanical and magnetic properties of MAEs (PDF)

AUTHOR INFORMATION

Corresponding Authors

Sergei S. Sheiko − *Department of Chemistry, University of North Carolina at Chapel Hill, Chapel Hill 27599, United States;* orcid.org/0000-0003-3672-1611; Email: sergei@email.unc.edu

Elena Yu. Kramarenko − *Faculty of Physics, Lomonosov Moscow State University, 119991 Moscow, Russian Federation; A.N. Nesmeyanov Institute for Organoelement Compounds, Russian Academy of Sciences, 119991 Moscow, Russian Federation;* orcid.org/0000-0003-1716-7010; Email: kram@polly.phys.msu.ru

Authors

Sergei A. Kostrov − *Faculty of Physics, Lomonosov Moscow State University, 119991 Moscow, Russian Federation; A.N. Nesmeyanov Institute for Organoelement Compounds, Russian Academy of Sciences, 119991 Moscow, Russian Federation*

Erfan Dashtimoghadam − *Department of Chemistry, University of North Carolina at Chapel Hill, Chapel Hill 27599, United States;* orcid.org/0000-0001-5607-7961

Andrew N. Keith − *Department of Chemistry, University of North Carolina at Chapel Hill, Chapel Hill 27599, United States;* orcid.org/0000-0001-6351-5392

Complete contact information is available at: https://pubs.acs.org/10.1021/acsami.1c12860

Author Contributions

S.A.K. conducted dynamic mechanical tests in the magnetic field and analyzed the obtained data; E.D. designed, synthesized, and characterized the macromonomers and polymer networks; A.N.K. performed stress−strain elongation mechanical tests and data analysis. E.Y.K. and S.S.S. were primary writers of the manuscript; E.Y.K. is the principal investigator. All authors discussed the results and provided feedback on the manuscript.

Notes

The authors declare no competing financial interest.

ACKNOWLEDGMENTS

This work was financially supported by the Russian Science Foundation (grant no. 19-13-00340). Access to electronic

https://doi.org/10.1021/acsami.1c12860
ACS Appl. Mater. Interfaces XXXX, XXX, XXX−XXX

scientific resources was provided by the Lomonosov Moscow State University and INEOS RAS with the support of Ministry of Science and Higher Education of the Russian Federation. S.S.S., A.K., and E.D. acknowledge funding from the National Science Foundation (DMR 1921835 and DMR 2004048). SEM investigation of MAEs was made using the equipment of the Collaborative Access Center "Center for Polymer Research" of ISPM RAS. We are grateful to Y.A. Alekhina for the magnetic measurements.

REFERENCES

(1) Vatankhah-Varnosfaderani, M.; Daniel, W. F. M.; Everhart, M. H.; Pandya, A. A.; Liang, H.; Matyjaszewski, K.; Dobrynin, A. V.; Sheiko, S. S. Mimicking biological stress-strain behaviour with synthetic elastomers. *Nature* **2017**, *549*, 497−501.

(2) Keith, A. N.; Vatankhah-Varnosfaderani, M.; Clair, C.; Fahimipour, F.; Dashtimoghadam, E.; Lallam, A.; Sztucki, M.; Ivanov, D. A.; Liang, H.; Dobrynin, A. V.; Sheiko, S. S. Bottlebrush bridge between soft gels and firm tissues. *ACS Cent. Sci.* **2020**, *6*, 413−419.

(3) Vatankhah-Varnosfaderani, M.; Keith, A. N.; Cong, Y.; Liang, H.; Rosenthal, M.; Sztucki, M.; Clair, C.; Magonov, S.; Ivanov, D. A.; Dobrynin, A. V.; Sheiko, S. S. Chameleon-like elastomers with molecularly encoded strain-adaptive stiffening and coloration. *Science* **2018**, *359*, 1509−1513.

(4) Daniel, W. F. M.; Burdyńska, J.; Vatankhah-Varnoosfaderani, M.; Matyjaszewski, K.; Paturej, J.; Rubinstein, M.; Dobrynin, A. V.; Sheiko, S. S. Solvent-free, supersoft and superelastic bottlebrush melts and networks. *Nat. Mater.* **2015**, *15*, 183−189.

(5) Filipcsei, G.; Csetneki, I.; Szilágyi, A.; Zrínyi, M. Magnetic Field-Responsive Smart Polymer Composites. *Oligomers—Polymer Composites—Molecular Imprinting*; Gong, B., Sanford, A. R., Ferguson, J. S., Eds.; Advances in Polymer Science; Springer: Berlin/Heidelberg, Germany, 2007; pp 137−189, ISBN 978-3-540-46830-1

(6) Kramarenko, E. Y.; Stepanov, G. V.; Stepanov, G. V.; Khokhlov, A. R. Magnetically Active Silicone Elastomers: Twenty Years of Development. *INEOS Open* **2019**, *2*, 178−184.

(7) Shamonin, M.; Kramarenko, E. Y. Highly Responsive Magneto-active Elastomers. *Novel Magnetic Nanostructures. Unique Properties and Applications*, 1st ed.; Domracheva, N., Caporali, M., Rentschler, E., Eds.; Elsevier: Amsterdam, Netherlands, 2018; pp 221−245. ISBN 978-0-12-813594-5.

(8) Ubaidillah; Sutrisno, J.; Purwanto, A.; Mazlan, S. A. Recent progress on magnetorheological solids: materials, fabrication, testing, and applications. *Adv. Eng. Mater.* **2015**, *17*, 563−597.

(9) Menzel, A. M. Tuned, driven, and active soft matter. *Phys. Rep.* **2015**, *554*, 1−45.

(10) Abramchuk, S.; Kramarenko, E.; Grishin, D.; Stepanov, G.; Nikitin, L. V.; Filipcsei, G.; Khokhlov, A. R.; Zrínyi, M. Novel highly elastic magnetic materials for dampers and seals: Part II. Material behavior in a magnetic field. *Polym. Adv. Technol.* **2007**, *18*, 513−518.

(11) Stoll, A.; Mayer, M.; Monkman, G. J.; Shamonin, M. Evaluation of highly compliant magneto-active elastomers with colossal magneto-rheological response. *J. Appl. Polym. Sci.* **2014**, *131*, 39793.

(12) Abramchuk, S. S.; Grishin, D. A.; Kramarenko, E. Y.; Stepanov, G. V.; Khokhlov, A. R. Effect of Homogeneous Magnetic Field on the Mechanical Behavior of Soft Magnetic Elastomers under Compression. Polymer Science. *Polym. Sci., Ser. A* **2006**, *48*, 138−145.

(13) Abramchuk, S.; Kramarenko, E.; Stepanov, G.; Nikitin, L. V.; Filipcsei, G.; Khokhlov, A. R.; Zrínyi, M. Novel Highly Elastic Magnetic Materials for Dampers and Seals I.: Preparation and characterization of the elastic materials. *Polym. Adv. Technol.* **2007**, *18*, 883−890.

(14) Li, Y.; Li, J.; Li, W.; Du, H. A state-of-the-art review on magnetorheological elastomer devices. *Smart Mater. Struct.* **2014**, *23*, 123001.

(15) Odenbach, S. Microstructure and rheology of magnetic hybrid materials. *Arch. Appl. Mech.* **2016**, *86*, 269−279.

(16) Stepanov, G. V.; Abramchuk, S. S.; Grishin, D. A.; Nikitin, L. V.; Kramarenko, E. Y.; Khokhlov, A. R. Effect of a Homogeneous Magnetic Field on the Viscoelastic Behavior of Magnetic Elastomers. *Polymer* **2007**, *48*, 488−495.

(17) Romeis, D.; Toshchevikov, V.; Saphiannikova, M. Effects of local rearrangement of magnetic particles on deformation in magneto-sensitive elastomers. *Soft Matter* **2019**, *15*, 3552−3564.

(18) Makarova, L. A.; Nadzharyan, T. A.; Alekhina, Y. A.; Stepanov, G. V.; Kazimirova, E. G.; Perov, N. S.; Kramarenko, E. Y. Magnetoactive elastomer as an element of a magnetic retina fixator. *Smart Mater. Struct.* **2017**, *26*, 095054−095064.

(19) Alekhina, Y. A.; Makarova, L. A.; Kostrov, S. A.; Stepanov, G. V.; Kazimirova, E. G.; Perov, N. S.; Kramarenko, E. Y. Development of magnetoactive elastomers for sealing eye retina detachments. *J. Appl. Polym. Sci.* **2019**, *136*, 47425.

(20) Mayer, M.; Rabindranath, R.; Börner, J.; Hörner, E.; Bentz, A.; Salgado, J.; Han, H.; Böse, H.; Probst, J.; Shamonin, M.; Monkman, G. J.; Schlunck, G. Ultra-soft PDMS-based magnetoactive elastomers as dynamic cell culture substrata. *PLoS One* **2013**, *8*, No. e76196.

(21) Semisalova, A. S.; Perov, N. S.; Stepanov, G. V.; Kramarenko, E. Y.; Khokhlov, A. R. Strong magnetodielectric effects in magneto-rheological elastomers. *Soft Matter* **2013**, *9*, 11318−11324.

(22) Dashtimoghadam, E.; Fahimipour, F.; Keith, A. N.; Vashahi, F.; Popryadukhin, P.; Vatankhah-Varnosfaderani, M.; Sheiko, S. S. Injectable Non-leaching Tissue-mimetic Bottlebrush Elastomers: A New Platform for Advancing Reconstructive Surgery. *Nat. Commun.* **2021**, *12*, 3961.

(23) Sheiko, S. S.; Dobrynin, A. V. Architectural Code for Rubber Elasticity: From Supersoft to Superfirm Materials. *Macromolecules* **2019**, *52*, 7531−7546.

(24) Levental, I.; Georges, P. C.; Janmey, P. A. Soft biological materials and their impact on cell function. *Soft Matter* **2007**, *3*, 299−306.

(25) Thieulin, C.; Pailler-Mattei, C.; Abdouni, A.; Djaghloul, M.; Zahouani, H. Mechanical and topographical anisotropy for human skin: Ageing effect. *J. Mech. Behav. Biomed. Mater.* **2020**, *103*, 103551.

(26) Payne, A. R. The dynamic properties of carbon black-loaded natural rubber vulcanizates. Part I. *J. Appl. Polym. Sci.* **1962**, *6*, 57−63.

(27) Bellan, C.; Bossis, G. Field dependence of viscoelastic properties of MR elastomers. *Int. J. Mod. Phys. B* **2002**, *16*, 2447−2453.

(28) An, H.; Picken, S. J.; Mendes, E. Nonlinear rheological study of magneto responsive soft gels. *Polymer* **2012**, *53*, 4164−4170.

(29) An, H.-N.; Picken, S. J.; Mendes, E. Direct observation of particle rearrangement during cyclic stress hardening of magneto-rheological gels. *Soft Matter* **2012**, *8*, 11995−12001.

(30) Mitsumata, T.; Ohori, S. Magnetic polyurethane elastomers with wide range modulation of elasticity. *Polym. Chem.* **2011**, *2*, 1063−1067.

(31) Sorokin, V. V.; Ecker, E.; Stepanov, G. V.; Shamonin, M.; Monkman, G. J.; Kramarenko, E. Y.; Khokhlov, A. R. Experimental Study of the Magnetic Field Enhanced Payne effect in Magneto-rheological Elastomers. *Soft Matter* **2014**, *10*, 8765−8776.

(32) Sorokin, V. V.; Belyaeva, I. A.; Shamonin, M.; Kramarenko, E. Y. Magnetorheological response of highly filled magnetoactive elastomers from perspective of mechanical energy density: Fractal aggregates above the nanometer scale? *Phys. Rev. E* **2017**, *95*, 062501.

(33) Krautz, M.; Werner, D.; Schrödner, M.; Funk, A.; Jantz, A.; Popp, J.; Eckert, J.; Waske, A. Hysteretic behavior of soft magnetic elastomer composites. *J. Magn. Magn. Mater.* **2017**, *426*, 60−63.

(34) Sorokin, V. V.; Stepanov, G. V.; Shamonin, M.; Monkman, G. J.; Khokhlov, A. R.; Kramarenko, E. Y. Hysteresis of the viscoelastic properties and the normal force in magnetically and mechanically soft magnetoactive elastomers: Effects of filler composition, strain amplitude and magnetic field. *Polymer* **2015**, *76*, 191−202.

(35) Belyaeva, I. A.; Kramarenko, E. Y.; Stepanov, G. V.; Sorokin, V. V.; Stadler, D.; Shamonin, M. Transient magnetorheological response of magnetoactive elastomers to step and pyramid excitations. *Soft Matter* **2016**, *12*, 2901−2913.

https://doi.org/10.1021/acsami.1c12860
ACS Appl. Mater. Interfaces XXXX, XXX, XXX−XXX

(36) Choi, S.-B.; Li, W.; Yu, M.; Du, H.; Fu, J.; Do, P. X. State of the art of control schemes for smart systems featuring magneto-rheological materials. *Smart Mater. Struct.* **2016**, *25*, 043001.

https://doi.org/10.1021/acsami.1c12860
ACS Appl. Mater. Interfaces XXXX, XXX, XXX−XXX